10th International Conference on

Steel and Aluminium Structures (ICSAS24)

Rio de Janeiro, Brazil, 5-7, June, 2024

NUMERICAL AND ANALYTICAL ASSESSMENT OF THE TUBULAR PERFOBOND SHEAR CONNECTORS

Keila L. B. SOUZA[a], Vinicius A. S. SARDINHA [a], André T. SILVA[b], Jose A. G. HENRIQUES[c], Luciano R. O. LIMA [b] and Monique C. RODRIGUES [b]

[a] Civil Engineering Post-Graduate Program, Faculty of Engineering, State University of Rio de Janeiro, Rio de Janeiro, Brazil
Emails: keila.souza@uerj.br, viniciusardinha@gmail.com

[b] Faculty of Engineering, State University of Rio de Janeiro, Rio de Janeiro, Brazil
Email: tenchini@eng.uerj.br, luciano@eng.uerj.br, monique.rodrigues@eng.uerj.br

[c] Construction Engineering Research Group, Faculty of Engineering Technology, Hasselt University, Hasselt, Belgium
Email: jose.gouveiahenriques@uhasselt.be

Keywords: Composite structures; Tubular perfobond shear connector; Finite element analysis.

Abstract. *In composite structures, the shear connector is responsible for ensuring the interaction between the materials and their transfer of efforts. Many connectors have been studied, including conventional perfobond, which has excellent resistance but sometimes has limited ductility. Thus, this paper aims to study a tubular cross-section shear connector in order to achieve great resistance, such as a conventional perfobond connector, and suitable slip capacity. The results revealed good mechanical performance, especially in terms of ductility. Varying the strength parameters of the materials improved the resistance of the connectors. However, when the diameter of the holes was increased, the resistance and ductility of the connector decreased. An analytical formulation was proposed, and its result was satisfactorily aligned with the numerical result.*

1 INTRODUCTION

Currently, the construction industry must respond to the challenge of quality while respecting tight deadlines and the economy. Composite solutions are examples of structures capable of satisfying this demand. These structures have become increasingly popular in several European countries, including the USA, Canada, and Australia, among other countries [1].

Steel-concrete composite structural systems have been widely used in recent decades, aiming to combine the high tensile strength of steel and the compressive strength of concrete. This structural system can be used in different types of buildings, such as multi-storey buildings, bridges and parking lots. Such structures are known for their numerous advantages, such as the possibility of expanding architectural options, the use of long spans, and the reduction in the sections of structural elements, resulting in less material and greater efficiency.

As it is widely known, the shear bond is fundamental to the efficiency of composite structural systems. Some researchers explain that it is essential to understand the interactions at the shear interface between the two constituent structural components [2]. The authors also point out that numerous studies have shown that without an effective bond at the interface, the components of the system act independently; with an effective shear bond, slip at the interface is prevented and, therefore, the components of the system work together in bending in a monolithic way.

Generally, the transfer of stress and shear resistance along steel-concrete contact surfaces is usually achieved by friction, mechanical processes or adhesion. This means that in order to ensure interaction between the two materials, it is necessary to use elements that transmit the forces from one to another. Mechanical means are the most common, known as shear connectors. The structural behaviour of composite sections is significantly affected by the mechanical performance of shear connectors.

Some normative codes have been created and updated regarding shear connectors, such as the Eurocode 4 [3], the ABNT NBR 8800 (2008) [4], the Japan Society of Civil Engineering [5], the American National Standard ANSI/AISC-360-16 [6], among others.

Due to the limitations of some connectors, others have been developed. Thus, many of them have been researched and employed, such as the stud, C profiles, conventional perfobond, and crestbond, among others, where the perfobond connector is one of the most usually chosen. It has stood out so much so that numerous variations have been proposed.

Although the perfobond connector has excellent mechanical performance, it sometimes fails to perform well in terms of ductility [7]. Therefore, this paper aims to present a tubular cross-section perfobond shear connector (TPC) in order to achieve good resistance, such as the perfobond connector, as well as adequate ductility.

2 DEVELOPMENT AND VALIDATION OF NUMERICAL MODELING

The numerical analyses in this paper were developed in Abaqus 6.14 [8] using the Explicit solver, as previously adopted by other authors [7], [9]. Besides, the semi-automatic mass scaling method in Abaqus/Explicit is adopted to achieve a balance between solution time and accuracy. This solver is excellent at solving nonlinear problems with large deformations, complicated interactions and complex nonlinear materials [10]. The authors suggest that the speed at which the load is applied should be strictly controlled to ensure that the kinetic energy is relatively small compared to the internal energy, which was done in this study.

2.1 Reference model: perfobond connector

The shear connector presented in this paper has a tubular cross-section. As no experimental results were found in the literature for connectors similar to it, results from the perfobond connectors previously studied by other authors [11] were adopted to validate the numerical modelling (Figure 1). The authors studied several perfobond type connectors, and two of them were selected for validation of the numerical modelling in this study, E-P-2F-120-28 and E-P-2F-120-52. The following subsections present the characteristics of the numerical modelling used to analyse the Perfobond connectors mentioned.

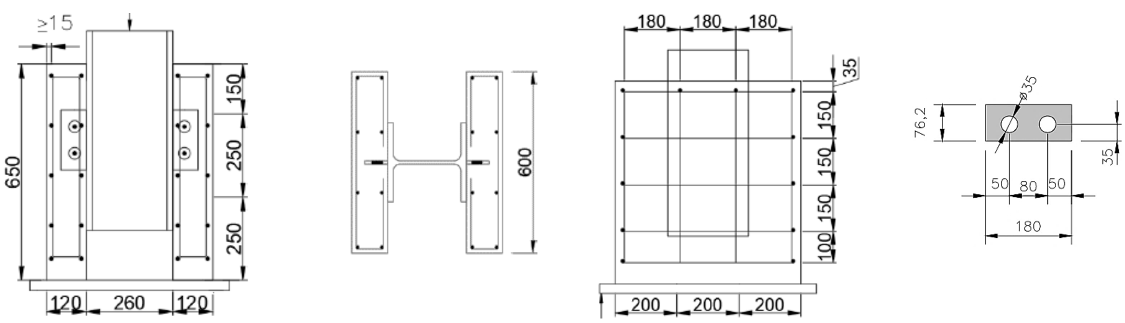

Figure 1:Geometry of Perfobond connector by Vianna *et al.* [11]

2.2 Geometry, finite element mesh, load and boundary conditions

The geometry of the specimens was based on Eurocode 4 [3], [11]. All components were modelled using solid elements, as defined in the experimental program.

In the simulation model, the three-dimensional eight-node reduced integration element (C3D8R) was introduced to simulate all components, concrete slabs, perfobond connector, steel beam and rebar. The slab and the steel beam adopted an 8 mm element size, while a mesh with an overall size of 5 mm and 24 mm was adopted for the shear connectors and rebars, respectively. The model contains 210.498 elements and 240.124 nodes.

Regarding the interactions and constraints, the general contact was considered for components in contact, such as steel profiles with slabs and connectors. Hard contact and penalty friction formulation were adopted for normal and tangential behaviour. A friction coefficient of 0.15 was assumed. The reinforcement rebars were embedded inside the concrete slab, so the embedded constraint was used to define the contact properly. The tie constraint was applied to simulate the weld between the shear connector and the steel beam in order to keep the faces connected during the entire numerical simulation.

The load was applied from the introduction of an axial displacement on the beam section's upper face. This displacement loading is slowly applied through a smooth amplitude function to reduce the dynamic effect of the inertial forces. The boundary conditions were defined as restrictions to the displacements in the three directions of the global axes at the slab bases. Both load and boundary conditions have been applied to the reference points belonging to the multi-point constraints (MPC). Figure 2 shows the geometry of the model, the finite element mesh, the application of loading, the boundary conditions (BC) and the embedded constraint.

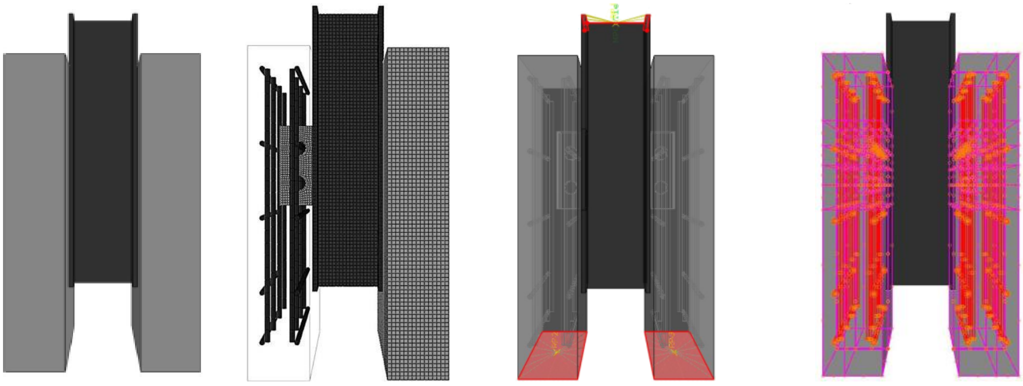

a. Geometry b. Mesh c. Load and BC d. Embedded

Figure 2: Characteristics of the numerical model

2.3 Material modelling

Similarly to the other definitions, the modelling of the materials followed the properties of the experimental tests. The concrete has f_{cm} equal to 28.30 MPa (28) and 51.90 MPa (52). A concrete damaged plasticity model (CDPM) was chosen to characterise the concrete behaviour. The application of this model concerns the definition of five plastic parameters to characterise the behaviour under compression, tension and the damage model. The parameters, dilation angle (ψ), eccentricity (ε), the ratio of biaxial to uniaxial compressive strength (f_{b0}/f_{c0}), the ratio of the second stress invariant on the tension meridian to that on the compressive (K) and a viscosity parameter (μ) are taken as 38, 0.1, 1.16, 0.667 e 0, respectively. To simulate the concrete's compressive and tensile behaviour, a stress-strain relationship containing sinusoidal and ,linear extensions, and a stress-crack opening relationship, respectively, were adopted. A damage formulation was adopted to complete the concrete modelling. The choices for modelling the behaviour of concrete were based on previous research [12].

Regarding steel materials, the stress-strain relationship for the rebars and the steel beam was modelled as elastic and perfectly plastic. At the same time, a quadrilinear curve was adopted to simulate the behaviour of the connector. The steel employed was S355, S275 and S500 for the connector, the beam and the rebar, respectively. It is important to mention that the steel modelling was also based on a previous study [12].

2.4 Validation of the numerical modelling

The developed FE model (N-P-2F-120-28 and N-P-2F-120-52) was validated by using the load per perfobond connector versus slip curves obtained from the experimental research (E-P-2F-120-28 and E-P-2F-120-52) [11] (Figure 3). The results are also presented in terms of the experimental ultimate load (P_{EXP}), numerical ultimate load (P_{NUM}), a comparison between the experimental and numerical (P_{NUM}/P_{EXP}), the average (*AV*), the standard deviation (*SD*) and the coefficient of variation (*CoV*) (Table 1).

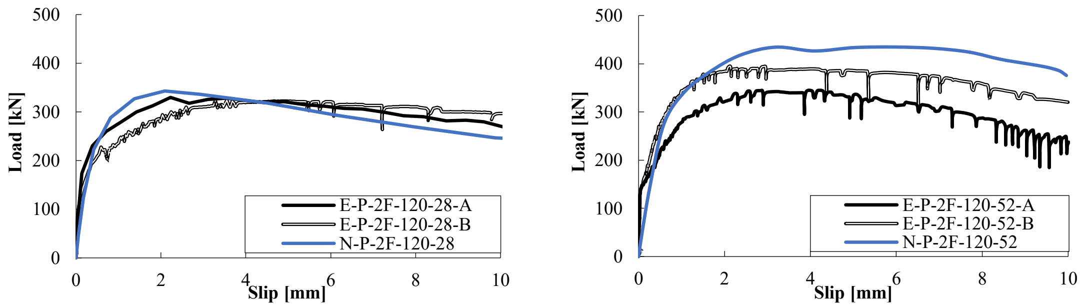

a. P-2F-120-28-A/B   b. P-2F-120-52-A/B

Figure 3: Load-slip: comparison from experimental and FEA

Table 1: Ultimate load: comparison from experimental and FEA results of perfobond connector

Model	f_{cm} (MPa)	P_{EXP} (kN)	P_{NUM} (kN)	P_{NUM}/P_{EXP}	AV	SD	CoV (%)
P-2F-120-28-A	28,30	329.55	342.94	1.04	1.12	0.10	8.97
P-2F-120-28-B		324.10		1.06			
P-2F-120-52-A	51,90	344.85	434.47	1.26			
P-2F-120-52-B		394.20		1.10			

From the observation of the obtained results, it can be seen that a satisfactory agreement was reached between both results, mainly for the model with 28,3 MPa. It could be observed that the N-P-2F-120-28 connector presented resistance up to 6% higher than the E-P-2F-120-28. About the models with 51,9 MPa, the N-P-2F-120-52 model was 10%-26% more resistant than the E-P-2F-120-52. However, when both experimental results are analysed, a difference of 14% between them could be observed. Despite the discrepancy observed between the numerical and experimental models, when analysing the behaviour of the load-slip curves, it can be seen that the stiffness and resistance of the N-P-2F-120-52 model reduced slowly after reaching its ultimate load, thus resembling the behaviour of the experimental models at this stage.

3 NUMERICAL ASSESSMENT OF TPC

3.1 Overview

It is believed that the closed cross-section will substantially contribute to the performance of the connector since the volume of concrete confined inside tends to be mobilised like the concrete cylinders in the hole, which have their share of contribution to the resistance capacity of a connector with holes. A numerical study will be carried out using numerical techniques similar to those previously validated to evaluate the viability of this connector.

In order to provide a basis for comparison with the perfobond connector mentioned [11], a tubular section with a similar cross-section area, 70x70x3.6, was adopted. The material properties were also preserved, as was the length of the connector, 180 mm, and the diameter of the hole, 35 mm. However, in order to investigate the influence of some parameters on the behaviour of the tubular perfobond connector (TPC), it was analysed other strengths for the connector, S275 and S450, another f_{cm}, 38 MPa, and other diameters for the connector hole, 30 mm and 40 mm.

3.2 Numerical modelling

As already mentioned, the characteristics of the validation presented were adopted for the TPC study. The only exceptions to the modelling presented are the geometry of the connector and the double symmetry constraint, where only a quarter of the specimen is simulated, which is widely adopted by a large number of researchers (Figure 4). Previously, the behaviour of models without symmetry and models with double symmetry was analysed, and no differences were found.

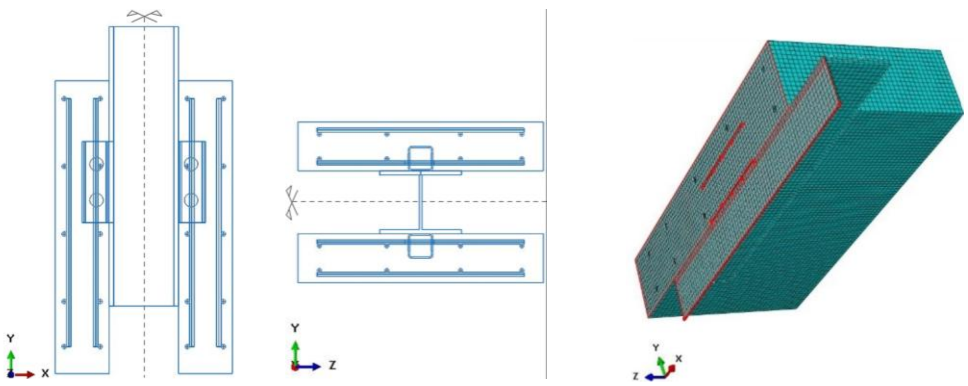

a. y-z plane b. x-z plane c. the model with double symmetry

Figure 4: Double symmetry constraints

3.3 Results of TPC

Concerning the nomenclature of the models, the index T70 indicates a tubular perfobond with a square section 70 x 70 x 3.6 mm. It is followed by the steel grades 275, 355 and 450 and the connector's hole diameters of 30 mm, 35 mm and 40 mm, respectively. Therefore, the concrete compressive strength is defined as 28, 38 and 52, respectively, corresponding to real values of 28.30, 38 and 51.90 MPa. For example, T70-355-D35-28 refers to an SHS connector model with an S355 steel grade, two holes with a diameter of 35 mm and concrete compressive strength f_{cm} equals 28.30 MPa.

Table 2 presents the results obtained in terms of the shear stiffness (K_s), the ultimate load (P), the characteristic resistance (P_{rk}), the slip capacity (δ_u), the characteristic slip capacity (δ_{uk}), the ductility factor (μ_d) following the procedure presented in [13], the ductility classification according to Eurocode 4 [3] and the failure modes. The analysed connectors performed extremely well in terms of resistance and ductility, which can be confirmed by the load-slip curves presented in Figure 5. Figure 6 shows the influence of the parameters on the resistance capacity of TPC, whose results are summarised in Table 3, where each influence was highlighted.

When the influence of the concrete strength was investigated, it was noticed that its increase generated gains of up to 13% in the TPC resistance capacity. It was also possible to observe that increasing the concrete strength provided ductility to the connector, leading to its peak load occurring at higher slip values.

Table 2: TPC results

Model	Ks (kN/mm)	P (kN)	P_{rk} (kN)	δ_u (mm)	δ_{uk} (mm)	μ_d	Ductile	Failure
T70-275-D35-28	566.12	333.39	300.05	21.16	19.04	6.93	Yes	B
T70-275-D35-38	518.50	385.05	346.54	20.62	18.56	4.88	Yes	A
T70-275-D35-52	626.29	404.91	364.42	18.44	16.59	3.92	Yes	A
T70-355-D30-28	582.03	380.59	342.53	11.97	10.77	4.00	Yes	B
T70-355-D30-38	623.42	408.80	367.92	15.56	14.00	5.13	Yes	B
T70-355-D30-52	659.61	460.96	414.87	17.82	16.04	3.95	Yes	A/B
T70-355-D35-28	581.51	368.91	332.02	13.44	12.09	4.61	Yes	B
T70-355-D35-38	629.56	411.48	370.33	10.75	9.68	3.00	Yes	B
T70-355-D35-52	661.76	447.62	402.85	15.39	13.85	3.55	Yes	A/B
T70-355-D40-28	553.98	354.89	319.40	11.99	10.79	4.60	Yes	B
T70-355-D40-38	576.30	401.65	361.48	12.17	10.95	3.36	Yes	B
T70-355-D40-52	626.68	439.49	395.54	15.91	14.31	3.27	Yes	A/B
T70-450-D35-28	589.46	391.28	352.16	8.99	8.09	4.75	Yes	C/B
T70-450-D35-38	631.49	424.00	381.60	13.97	12.57	5.43	Yes	C/B
T70-450-D35-52	670.09	473.24	425.92	12.43	11.19	3.48	Yes	C/B

*A - connector. B - concrete crushing. C - concrete cracking due to shear.

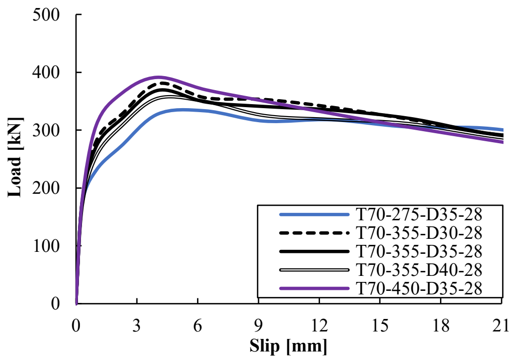

a. Models with 28.3 MPa

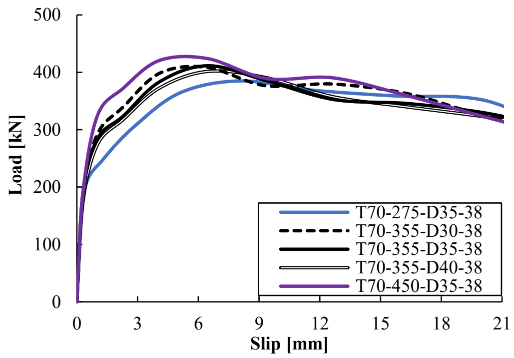

b. Models with 38 MPa

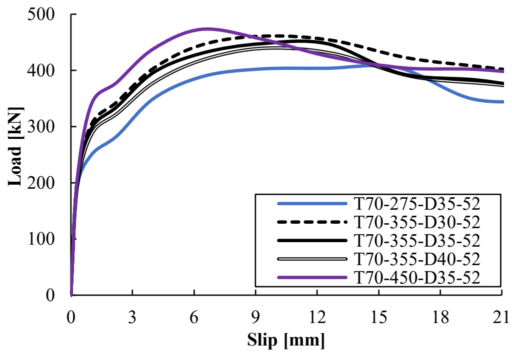

c. Models with 51.9 MPa

Figure 5: Load-slip of TPC

The influence of the connector steel grade was also evaluated. It is important to mention that when a higher strength was adopted, the ultimate capacity of the TPC increased by 11%, and this influence was more pronounced when the strength was changed from S275 to S355. Some authors warn that this influence on the strength of the connector is only effective for connectors with a yield stress of up to 400 MPa [14]. Unfortunately, increasing the connector strength leads to a decrease in its ductility and contributes to the concrete slab becoming the element most susceptible to failure. Furthermore, its peak load occurs at lower slip levels.

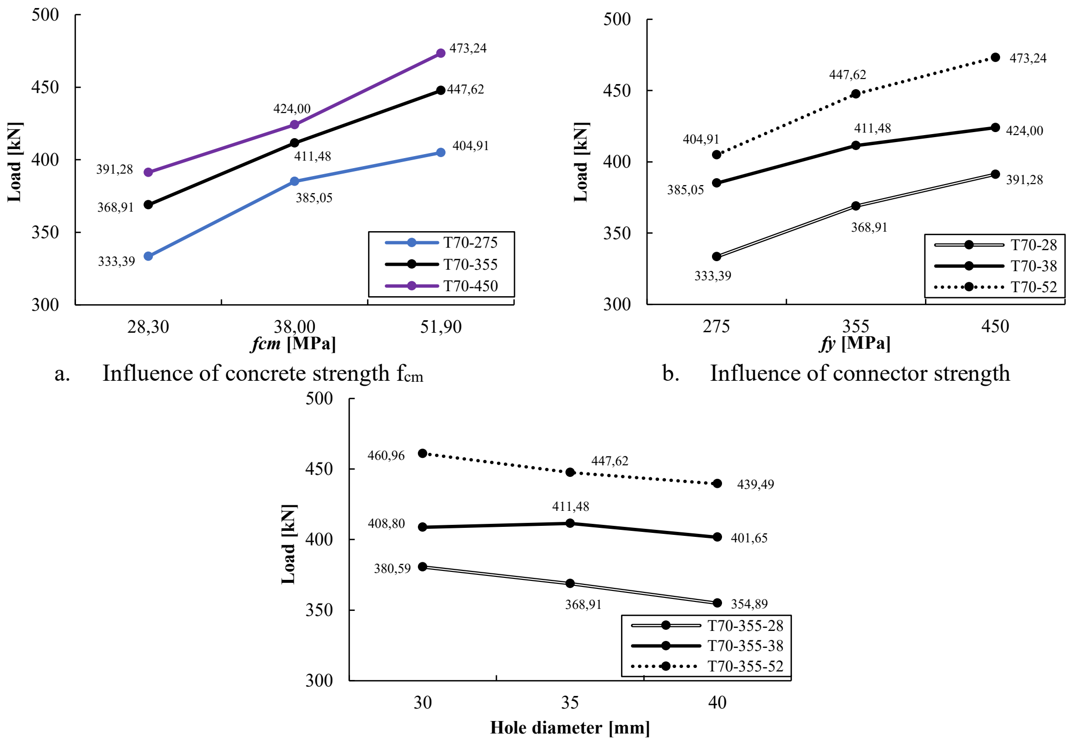

a. Influence of concrete strength f_{cm}

b. Influence of connector strength

c. Influence of hole diameter

Figure 6: Influence of parameters

Table 3: Summary of the parameters' influence

Parameter	Variation	Influence on resistance	Influence on slip
Concrete - f_{cm}	34%	7% – 15%	-20% – 55%
	37%	9% – 13%	-11% – 43%
Connector - f_y	31%	7% – 11%	-48% – -17%
	27%	3% – 6%	-33% – 30%
Hole diameter	17%	-3% – 1%	-31% – 12%
	14%	-4% – -2%	-11% – 13%

Although many authors [9], [15] consider that increasing the hole diameter improves the resistance and stiffness of shear connectors, this was not observed in the TPC. As ductility is an important aspect in the study of TPC, another way of evaluating ductility has been adopted. The ductility factor is used to facilitate the assessment of the inelastic behaviour of connectors. According to some authors [16], it must be at least equal to 2 to guarantee that the connectors have a truly ductile behaviour, which is the case of the TPC studied. Regarding the failure modes, most models failed by the concrete crushing, which is not interesting due to their brittle failure. Briefly, when the concrete strength is increased to 52 MPa, the failure occurs in the connector, as expected. When the strength of the connector is varied to its lowest value, failure occurs in the connector, with the exception of the T70-275-D35-28 model. When the strength varies to its highest value, failure occurs in concrete, where cracking occurs due to shear.

4 ANALYTICAL EVALUATION PROPOSAL FOR TUBULAR CONNECTOR

An analytical formulation was proposed with the aim of predicting the shear resistance of the proposed tubular connector. This formulation considers the geometry of the connector, the number of holes, the holes' diameter, the concrete slab compressive strength and the connector steel grade. It is important to mention that the parameters considered were based on previous research [17], and the necessary adjustments were applied to the angular and linear coefficients through the linear regression method using the numerical results discussed in the last section.

The methodology of the formulation is based on isolating the three possible failure modes of the system, i.e., connector yielding, concrete crushing and shear concrete cracking, obtaining a parcel of resistance for each failure mode. Hence, the small value between these three resistances determines the connector's ultimate load and the respective failure mode.

Equation (1) presents the formulation for assessing the resistance for the connector failure, while Equations (3) and (4) characterise the crushing and cracking failure modes, respectively.

$$F_{connector} = 1.6214\left(\frac{f_y\, A_{cc}\, 10^{-3}}{\sqrt{3}}\right) + 209{,}9 \quad (1)$$

$$A_{c_c} = (L_c - 2\phi)\, 2t_w \quad (2)$$

$$F_{crushing} = 13.535\left(\frac{\sqrt{\frac{h}{h_c}}\, {f_{cm}}^2\, h\, t_w\, 10^{-3}}{\phi}\right) + 300{,}46 \quad (3)$$

$$F_{cracking} = 48.455\left(\frac{E_{CS}\, A_{cs}\, 10^{-7}\ 2\phi}{h}\right) - 362.63 \quad (4)$$

$$A_{c_s} = h\,(L_c - 2\phi) \quad (5)$$

$$F = \min\,(F_{connector};\ F_{crushing};\ F_{cracking}) \quad (6)$$

where L_c is the connector length, ϕ is the hole diameter, t_w is the connector thickness, A_{cc} is the shear connector area, f_y is the connector yield stress, f_{cm} is the concrete compressive strength, h is the concrete slab height, h_c is the connector height, E_{cs} is the concrete secant modulus, and A_{cs} is the concrete shear area.

Table 4 summarises the results of the proposed method, where $F_{connector}$, $F_{crushing}$ and $F_{cracking}$ are the resistance associated with tubular connector, concrete crushing and cracking failure modes, respectively, and F is the adopted shear resistance corresponding to the lowest value of the three resistances mentioned above. The failure mode from the analytical method is also presented, as well as the ultimate resistance and failure mode obtained from numerical modelling. Finally, the average (*AV*) and coefficient of variation (*CoV*) of the ratio between numerical and analytical formulation resistances are also presented in order to improve comprehension of the comparison of the result.

There was a satisfactory approximation of the obtained results through the equations presented with the results from the numerical modelling, which resulted in a maximum 9% difference. The statistical results corroborated the effectiveness of the proposed equations, where the average was 1.01, a value very close to the unit, and the *CoV* of 3.79% indicated low variability in the results. Moreover, the effectiveness can also be assessed through the good correlation between the failure observed in the numerical models and those determined using the proposed analytical formulation.

Table 4: Shear resistance and failure modes according to the proposed formulation

Model	Analytical					Numerical		$\frac{F_{NUM}}{F}$
	$F_{connector}$ (kN)	$F_{crushing}$ (kN)	$F_{cracking}$ (kN)	F (kN)	Failure mode	F_{NUM} (kN)	Failure mode	
T70-275-D35-28	413.79	358.81	492.26	358.81	B	333.39	B	0.93
T70-275-D35-38	395.25	407.94	577.75	395.25	A	385.05	A	0.97
T70-275-D35-52	395.25	451.18	720.23	395.25	A	404.91	A	1.02
T70-355-D30-28	461.13	368.54	436.75	368.54	B	380.59	B	1.03
T70-355-D30-38	461.13	425.85	516.68	425.85	B	408.80	B	0.96
T70-355-D30-52	461.13	476.30	649.91	461.13	A	460.96	A/B	1.00
T70-355-D35-28	449.17	358.81	492.26	358.81	B	368.91	B	1.03
T70-355-D35-38	449.17	407.94	577.75	407.94	B	411.48	B	1.01
T70-355-D35-52	449.17	451.18	720.23	449.17	A	447.62	A/B	1.00
T70-355-D40-28	437.21	351.52	525.56	351.52	B	354.89	B	1.01
T70-355-D40-38	437.21	394.50	614.38	394.50	B	401.65	B	1.02
T70-355-D40-52	437.21	432.34	762.42	432.34	B	439.49	A/B	1.02
T70-450-D35-28	513.20	358.81	492.26	358.81	B	391.28	C/B	1.09
T70-450-D35-38	513.20	407.94	577.75	407.94	B	424.00	C/B	1.04
T70-450-D35-52	513.20	451.18	720.23	451.18	B	473.24	C/B	1.05
							AV	1.01
							***CoV* (%)**	3.79

5 CONCLUSIONS

This paper evaluated the performance of a perfobond tubular shear connector as a function of some properties of its main constituent materials, as well as characteristics related to the connector geometry. Thus, the main conclusions obtained were:

- Regarding the validation carried out with the perfobond connector, it was noted that there is still a need to improve the accuracy of the numerical models. However, there was an adequate approximation in terms of ultimate load, especially with regard to the 28 MPa model.
- The TPC performed adequately in terms of both resistance and ductility. Furthermore, all the connectors studied are ductile, according to Eurocode 4 [3].

- Increasing the concrete strength gave substantial increments in the shear resistance of the connectors, as well as in their ductility. Increasing the strength of the connector steel also had a positive influence on its resistance but did not contribute to its ductility.
- Despite the opinion of many authors, the performance of the connector studied was not positively influenced by increasing the hole diameter.
- In a brief comparison with the perfobond connector, the TPC performs well, achieving shear resistance capacity up to 7.6% higher and also presenting good ductile behaviour.
- Analytical formulations were presented to determine the shear resistance capacity based on the failure mode. Further studies are needed to refine the proposed equations, but these formulations provided excellent correlations with the results obtained by the numerical models.

ACKNOWLEDGEMENTS

The authors would like to thank CAPES (Finance code 001), CERG, CNPq (303365/2019-6, 305047/2023-0, 406617/2023-6) and FAPERJ (E-26/211.186/2021, E-26/201.250/2021; E-26/200.315/2023, E-26/200.315/2023) for the financial support given to this research program.

REFERENCES

[1] Patil, P.S., Shaikh, M.G., *'A Study of Effect of Shear Connector in Composite Beam in Combined Bending and Shear by Ansys', International Journal of Innovative Technology and Exploring Engineering*, 3, 67-74, 2013.

[2] Vella, N., Kyvelou, P., Buhagiar, S., Gardner, L., *'Innovative shear connectors for composite cold-formed steel-timber structures: An experimental investigation', Engineering Structures*, 287, 116120, 2023.

[3] *Design of composite steel and concrete structures – Part 1-1: General rules and rules for buildings*. EN 1994-1-1, Brussels, Belgium, European Committee for Standardization, 2004.

[4] *Desing of steel and composite structures for buildings*. ABNT NBR 8800, Rio de Janeiro, Brazil, Brazilian Association of Technical Standards, 2008.

[5] *Standard Specifications for Steel and Composite Structures*. JSCE, Tokyo, Japan, Japan Society of Civil Engineers, 2009.

[6] *Specification for Structural Steel Buildings*. ANSI/AISC-360-16, Chicago, United States of America, American National Standard Institute – American Institute of Steel Construction, 2016.

[7] Spremić, M., Gluhović, N., Marković, Z., Dobricć, J., Filipović, A., *'Comparison of headed studs with perfobond shear connectors - experimental and numerical analysis', Proceedings of Eurosteel 2017*, Copenhagen, Denmark, 2237-2246, 2017.

[8] ABAQUS *Analysis user's manual. 6.14th ed.* Rhode Island, United States of America, ABAQUS Inc S. *Dassault Systèmes Simulia Corp*. *Johnston*, 2014.

[9] Zheng, S., Liu, Y., Yoda, T., Lin, W., *'Parametric study on shear capacity of circular-hole and long-hole perfobond shear connector', Journal of Constructional Steel Research,* 117, 64–80, 2016.

[10] Gu, J. C., Liu, D., Deng, W. Q., Zhang, J. D., *'Experimental study on the shear resistance of a comb-type perfobond rib shear connector', Journal of Constructional Steel Research,* 158, 279–289, 2019.

[11] Vianna, J. da C., Andrade, S. A. L., Vellasco, P. C. G., Costa-Neves, L. F., *'Experimental study of Perfobond shear connectors in composite construction', Journal of Constructional Steel Research,* 81, 62–75, 2013.

[12] Souza, K. L. B., Silva, A. T., Henriques, J., Vellasco, P. C. G. S., Rodrigues, M. C., '*Numerical analysis of proposed tubular perfobond shear connector'*, P*roceedings of the XIV International Conference on Metal Structures*, Poznań, Poland, 2021.

[13] Arévalo, D., Hernández, L., Gómez, C., Velasteguí, G., Guaminga, E., Baquero, R., Dibujés, R., *'Structural performance of steel angle shear connectors with different orientation', Case Studies in Construction Materials,* 14, e00523, 2021.

[14] Yu, Z., He, S., Mosallam, A. S., Jiang, S., Feng, W.' *Experimental and numerical evaluation of perfobond rib shear connectors embedded in recycled aggregate concrete', Hindawi, Advances in Civil Engineering,* 2020, 2020.

[15] Zhao, C., Liu, Y., Zheng, S., Shinichi, H., Yamaguchi, K., *'Experimental analysis of shear behavior of oval perfobond connector', Proceedings of ICTE 2011: International Conference on Tissue Engineering,* Lisbon, Portugal, ASCE, 1983-1988, 2011.

[16] Kwon, G., Engelhardt, M. D., Klingner, R. E., *'Parametric studies and preliminary design recommendations on the use of postinstalled shear connectors for strengthening noncomposite steel bridges', Journal of bridge engineering,* 17, 310–317, ASCE, 2012.

[17] Costa, F. S. S., *'Estudo numérico dos conectores T-Perfobond com mesa não soldada em vigas mistas de aço e concreto'*, Master thesis – Faculdade de Engenharia, Universidade do Estado do Rio de Janeiro, Rio de Janeiro, 2023.